Environ Sci Pollut Res (2017) 24:18470–18478
DOI 10.1007/s11356-017-9310-0

RESEARCH ARTICLE

Photochemical generation of reactive intermediates from urban-waste bio-organic substances under UV and solar irradiation

Marcela Prado Silva[1,2] · Arlen Mabel Lastre-Acosta[1] · Simón Mostafa[3] · Garrett McKay[3] · Karl G. Linden[3] · Fernando L. Rosario-Ortiz[3] · Antonio Carlos Silva Costa Teixeira[1]

Received: 20 February 2017 / Accepted: 18 May 2017 / Published online: 23 June 2017

Abstract Singlet oxygen ($^1O_2$), hydroxyl radicals ($^•OH$), and excited triplet states of organic matter ($^3OM^*$) play a key role in the degradation of pollutants in aquatic environments. The formation rates and quantum yields (Φ) of these reactive intermediates (RI) through photosensitized reactions of dissolved organic matter (DOM) have been reported in the literature for decades. Urban biowaste-derived substances (UW-BOS), a form of organic matter derived from vegetative and urban waste, have recently been shown to be efficient sensitizers in the photo-degradation of different contaminants. Nevertheless, no quantitative measurements of photo-oxidant generation by UW-BOS have been reported. In this study, the formation quantum yields of $^1O_2$ and $^•OH$, as well as quantum yield coefficients of TMP degradation (indicative of $^3OM^*$ formation), were quantified for two UW-BOS samples, under 254-nm UV radiation or simulated sunlight and compared to a DOM standard from the Suwanee River (SRNOM). Values of Φ for UW-BOS samples ranged from $\Phi(+^1O_2) = 8.0$ to 8.8×10^{-3}, $\Phi(+^•OH) = 4.1$ to 4.3×10^{-6}, and $f_{TMP} = 1.22$ to 1.23×10^2 L Einstein^{-1} under simulated sunlight and from $\Phi(+^1O_2) = 1.4$ to 2.3×10^{-2}, $\Phi(+^•OH) = 1.3$ to 3.5×10^{-3}, and $f_{TMP} = 3.3$ to 3.9×10^2 L Einstein^{-1} under UV. Although UW-BOS are not necessarily better than natural DOM regarding photosensitizing properties, they do sensitize the production of RI and could potentially be used in engineered treatment systems.

Keywords Urban-waste bio-organic substances · Reactive intermediates · Photo-oxidation processes · Quantum yield · UV radiation · Simulated sunlight amicarbazone · Aquatic environments

Responsible editor: Vítor Pais Vilar

Electronic supplementary material The online version of this article (doi:10.1007/s11356-017-9310-0) contains supplementary material, which is available to authorized users.

✉ Marcela Prado Silva
marpradosilva@hotmail.com

[1] Chemical Engineering Department, University of São Paulo, Av. Prof. Luciano Gualberto, tr. 3, 380, São Paulo, Brazil

[2] Graduate Program on Environment and Regional Development, University of Oeste Paulista, Raposo Tavares, km 572, Bairro do Limoeiro, Presidente Prudente, São Paulo, Brazil

[3] Civil, Environmental and Architectural Engineering Department, University of Colorado, 428 UCB, Boulder, CO 80309, USA

Introduction

The occurrence of contaminants of environmental concern (CEC) in surface waters has been extensively reported (Bound and Voulvoulis 2004; Emblidge and De Lorenzo 2006; Vecchiato et al. 2015). These compounds have the potential to impact human and ecosystem health (U.S. Environmental Protection Agency 2016), and therefore, their fate and transport in environmental systems is of interest to scientists and engineers. Photochemical processes, such as direct and sensitized (or indirect) photolysis, are important mechanisms for the degradation of CEC in both natural and engineered aquatic systems (Schwarzenbach et al. 2003; Vione et al. 2010).

Through direct photolysis, pollutants react by absorbing light and ultimately undergoing degradation. The efficacy of this process depends on the overlap between the light spectrum, the absorption spectra of the contaminants, and their degradation quantum yields (Braun et al. 1991; Lester et al. 2013; Schwarzenbach et al. 2003). Indirect photolysis

involves the degradation of the CEC via reactions with reactive intermediates (RIs). The RIs of environmental importance include singlet oxygen ($^1O_2$), hydroxyl radicals ($^{\bullet}OH$), and triplet-excited states ($^3OM^*$) (Rosario-Ortiz and Canonica 2016). These RIs are mainly formed by photosensitization of dissolved organic matter (DOM) (Vione et al. 2010). Light absorption by DOM leads to the formation of triplet-excited states ($^3OM^*$) by intersystem crossing following the formation of singlet-excited states ($^1OM^*$) (Mostafa et al. 2014). Energy transfer between $^3OM^*$ and triplet-state molecular oxygen ($^3O_2$) forms $^1O_2$ (Passananti et al. 2014). The formation of $^{\bullet}OH$ is less clear. It is known that $^{\bullet}OH$ can form via photolysis of nitrate and nitrite; however, photolysis of DOM also forms $^{\bullet}OH$ and other species which can also behave like $^{\bullet}OH$ (McKay and Rosario-Ortiz 2015; Rosario-Ortiz and Canonica 2016; Vione et al. 2014). There have been numerous reports on the quantification of quantum yields for the production of these RIs from DOM samples and also wastewater-derived organic matter (Haag et al. 1984; Lester et al. 2013; McKay and Rosario-Ortiz 2015; Cawley et al. 2015; Dalrymple et al. 2010, Zhang et al. 2014, Zhou et al. 2017).

Despite the production of RI from naturally occurring DOM, the kinetics of contaminant degradation under typical (low) DOC concentrations is slow (t1/2, minutes~hours) (Avetta et al. 2013; Gomis et al. 2014). Alternatively, urban biowaste-derived sensitizing materials contain soluble bio-organic substances (UW-BOSs), which exhibit similar physicochemical properties to DOM and have been reported as promising chemical auxiliaries for a number of technological applications including environmental remediation processes (Avetta et al. 2015).

UW-BOSs are described as mixtures of macromolecules with average molecular weight ranging from 67 to 463 kg mol^{-1} (Avetta et al. 2012). Chemical composition data also show that UW-BOS are macromolecules combining a complex lignin-derived structure with several functionalities and carbon types of different polarities, formed by long aliphatic carbon chains substituted by aromatic rings and functional groups such as COOH, CON, C=O, PhOH, O-alkyl, O-aryl, OCO, OMe, and NRR′, (R and R' = alkyl or H) (Prevot et al. 2011). Structural similarities between UW-BOS and natural organic matter (NOM) are expected. In fact, according to Avetta et al. (2012), UW-BOSs are the likely remains of the main constituents of the sources of bio-organic refuse that were not completely mineralized during aging under aerobic fermentation conditions. Detailed information on the composition and functional groups of different UW-BOSs can be found elsewhere (Arques and Prevot 2015). Regarding safety, previous acute toxicity assays indicated the absence of harmful effects to the test-organism *Vibrio fischeri* after adding UW-BOS to water (Avetta et al. 2012; Avetta et al. 2013). Nevertheless, toxicity assays with organisms from different trophic levels are still needed.

The capability of UW-BOS to promote the photodegradation of various pollutants has been studied, and several encouraging results have been obtained (Avetta et al. 2013; Avetta et al. 2015; Avetta et al. 2012; Prevot et al. 2011, 2010). Most of these studies focus on the implementation of photo-Fenton processes at circumneutral conditions, possible through the stabilization of iron species in the presence of UW-BOS, while few studies demonstrated the involvement of reactive oxygenated species in the elimination of different contaminants in the presence of UW-BOS. Prevot et al. (2010) showed a relevantly lower dye abatement rate in the presence of pure N_2 compared to air, which suggests a reaction mechanism involving $^{\bullet}OH$ and $^1O_2$. Prevot et al. (2011) monitored these species during the degradation of 4-chlorophenol in the presence of UW-BOS by EPR spectroscopy, concluding that UW-BOS are potential photosensitizers for applications in environmental remediation. However, quantitative measurements of RI generated by UW-BOS are presently unavailable.

We addressed this knowledge gap by measuring the quantum yields of $^1O_2$ and $^{\bullet}OH$ formation, as well as quantum yield coefficients of TMP degradation (indicative of $^3OM^*$ formation) for two UW-BOS samples, both under ultraviolet irradiation (UV) at 254 nm and solar-simulated light. This quantitative information is critical for assessing the potential of these materials in photochemical wastewater treatment. Quantum yield values were compared with those obtained for a standard organic matter Suwannee River Natural Organic Matter (SRNOM). Additionally, we investigated the effect of UW-BOS on the degradation of amicarbazone (AMZ), a herbicide extensively used in large-scale cultivations and a potential emerging concern water pollutant.

Experimental

Chemicals

All solutions were prepared using water purified by reverse osmosis (Milli-Q). Technical grade amicarbazone (AMZ, 241.3 g mol^{-1}, minimum purity 95.4%) was supplied by Arysta LifeScience Corp. and used as a standard in liquid chromatography (HPLC) analysis and in photochemical experiments. SRNOM was obtained from the International Humic Substances Society (catalog number 1R101N).

Two UW-BOS samples, identified by the acronyms CVT230 and CVDF110, were obtained from the process lines of ACEA Pinerolese waste treatment plant in Pinerolo (Italy) and have been isolated from different source materials: CVT230 from home gardening and park trimming residue (GR) piles aerated for 230 days and CVDF110 from 35/55/10 *w/w/w* urban waste organic humic fraction/GR/urban sewage sludge mix aerated for 110 days.

SRNOM and UW-BOS were dissolved in 10 mmol L^{-1} phosphate buffer (pH 7.2) at a concentration of 10 mg L^{-1}. Bovine catalase (Sigma Aldrich), furfuryl alcohol-FFA (TCI America), para-chlorobenzoic acid-pCBA (ICN Biomedicals Inc.), 2,4,6-trimethylphenol-TMP (Sigma Aldrich), benzene (Alpha Aesar), sodium nitrate and sodium phosphate (Fisher Scientific), and phosphoric acid (85%, J.T. Baker) were all of reagent grade purity. For HPLC analysis, acetonitrile (HPLC grade) and methanol (HPLC grade) were purchased from Honeywell.

Irradiation apparatus

Solar simulation experiments were conducted using a Model 94041 Oriel solar simulator equipped with a 1000-W lamp and air mass 1.5 global filter (Newport Corp.). The total irradiance was 68 W m^{-2} in the wavelength range 290–400 nm. Solar simulator irradiance was measured with a USB2000 spectroradiometer (Ocean Optics Inc.). Samples were irradiated in 2-mL pyrex vials with no headspace and exposed to radiation while in a water bath maintained at 20 °C.

Irradiation by a low-pressure (LP) UV lamp was performed using a semi-collimated beam apparatus with four 15-W LP lamps (ozone-free, General Electric #G15 T8), emitting at 254 nm. Petri dishes (70 × 50 mm) were used as exposure vessels in which the samples were continuously stirred. A radiometer (International Light Inc., Model 1700/SED 240/W) was used to measure UV irradiance at the surface of the liquid samples; the incident irradiance was 2.00 mW cm^{-2}.

Measurements and calculation of apparent quantum yields

Furfuryl alcohol (FFA) was used as a chemical probe to measure the formation of $^1O_2$ from NOM (SRNOM or UW-BOS)-containing solutions, following previously established procedures (Mostafa and Rosario-Ortiz 2013) for both LP-UV and simulated sunlight systems, since FFA is commonly used to measure $^1O_2$ formation at wavelengths >300 nm, and its direct photolysis at 254 nm can be considered insignificant for UV experiments (Lester et al. 2013). FFA was added to the samples at an initial concentration of 22.5 μmol L^{-1} and its concentration was monitored after light exposure using liquid chromatography. Methanol (0.1 mol L^{-1}) was added in order to quench photochemically generated $^{\bullet}OH$ radicals, in order not to overestimate $^1O_2$ concentration; the reaction between FFA and $^{\bullet}OH$ radicals follow a second-order rate law with $k_{\bullet OH,FFA}$ = 1.5 × 10^{10} L mol^{-1} s^{-1} (Mostafa and Rosario-Ortiz 2013).

Samples were exposed over 4 h under simulated sunlight and over 1 h under the LP-UV lamp. Plotting $\ln[FFA]/[FFA]_0$ versus irradiation time generates a straight line as expected from a pseudo-first-order reaction. The slope obtained is divided by the second-order reaction rate constant between $^1O_2$ and FFA (1.2 × 10^8 L mol^{-1} s^{-1}) according to Haag et al. (1984) to obtain the steady-state singlet oxygen concentration, $[^1O_2]_{ss}$. This value was used to determine the $^1O_2$ formation quantum yield [$\Phi(+^1O_2)$], according to Eq. 1:

$$\left[{}^1O_2\right]_{ss} = \frac{R_a\,\Phi\left(+{}^1O_2\right)}{\Sigma k_{1O2,X}[X] + k_{d,H2O}} \quad (1)$$

where R_a is the rate of light absorption by DOM over the wavelength range, which is a function of the solution absorbance and irradiance; $k_{1O2,X}$ is the second-order reaction rate constant between $^1O_2$ and any species X present in the water matrix (including but not limited to NOM); and $k_{d,H2O}$corresponds to the rate constant of $^1O_2$ decay to the ground state due to physical quenching by water molecules ($k_{d,H2O}$ = 2.5 × 10^5 s^{-1}) (Mostafa and Rosario-Ortiz 2013). The overall decay of singlet oxygen is dominated by $k_{d,H2O}$ in such a way that the physical or chemical quenching due to OM or other species ($k_{1O2,X}[X]$) can generally be ignored at environmentally relevant concentrations (Mostafa and Rosario-Ortiz 2013). R_a is calculated by Eq. 2:

$$R_a = \int \frac{E_P^0\left(1-10^{-Abs_\lambda z}\right)}{z}\,d\lambda \quad (2)$$

where $E_P{}^0$ is the irradiance (measured with an Ocean Optics USB2000 spectroradiometer), Abs_λ is the solution absorbance at wavelength λ, and z is the optical path length.

For the LP-UV-irradiated systems, the formation quantum yield of hydroxyl radicals [$\Phi(+^{\bullet}OH)$] from DOM (SRNOM or UW-BOS)-containing solutions was measured using para-chlorobenzoic acid (pCBA) as a chemical probe. The choice of this method was based on the higher photostability of pCBA at 254 nm in comparison with other probe molecules, like phenol (Lester et al. 2013). In brief, pCBA was added to the samples at an initial concentration of 2.23 × 10^{-2} mmol L^{-1} and the solution was exposed to UV irradiation for up to 1 h. The slope of a plot of $\ln[pCBA]/[pCBA]_0$ as a function of irradiation time yielded k_{pCBA}, assuming pseudo-first-order pCBA concentration decay. The value of $\Phi(+^{\bullet}OH)$ at 254 nm was then estimated as R_{pCBA}/R_a, where R_{pCBA} corresponds to the initial pCBA degradation rate ($R_{pCBA} = k_{pCBA}[pCBA]_0$), and R_a is the rate of UV radiation absorbed by DOM at 254 nm.

For the simulated sunlight-irradiated systems, the formation rate of $^{\bullet}OH$ radicals ($R^f_{\bullet OH}$) from DOM (SRNOM or UW-BOS)-containing solutions was measured using the Dorfman reaction (Dorfman et al. 1962), i.e., the hydroxylation of benzene to phenol. Briefly, a 10-mg L^{-1} DOM (SRNOM or UW-BOS) solution was spiked with 3 mmol L^{-1} benzene and irradiated for 4 h, with samples collected every hour. $R^f_{\bullet OH}$ was calculated based on the rate of phenol production divided by the known reaction yield

(0.63), as detailed elsewhere (McKay and Rosario-Ortiz 2015). The corresponding formation quantum yields were obtained by dividing $R^f_{\bullet OH}$ by the rate of light absorption by DOM over the wavelength range (R_a). To quantify $^{\bullet}OH$ formation due solely to UW-BOS or NOM (and not photo-Fenton processes), catalase (20 U mL^{-1}) was added to each sample 30 min before irradiation. Catalase decomposes photochemically generated H_2O_2 and (the minor amount) produced as a byproduct of benzene hydroxylation (Larson and Zepp 1988).

For both LP-UV and simulated sunlight systems, TMP was used as a probe to assess the formation of $^3OM^*$; its degradation is an indicative of $^3OM^*$ formation (Mostafa et al. 2014; Cawley et al. 2015; Canonica and Freiburghaus 2001; Cawley et al. 2009; Richard et al. 2004; Golanoski et al. 2012). TMP was spiked at an initial concentration of 3.67×10^{-3} mmol L^{-1} into DOM (SRNOM or UW-BOS)-containing solutions, which were irradiated under LP-UV (1 h) or simulated sunlight (4 h). Direct photolysis of TMP at 254 nm and above was found to be slow (Lester et al. 2013). The quantum yield coefficient f_{TMP} (L $Einstein^{-1}$), was calculated according to previous studies (Sharpless et al. 2014; McCabe and Arnold 2016; McKay et al. 2017), as the TMP degradation rate constant (k_{TMP}) divided by the rate of light absorption by DOM over the wavelength range (R_a) [$f_{TMP} = k_{TMP}/R_a$, L $Einstein^{-1}$]. The slope of a plot of $\ln[TMP]/[TMP]_0$ as a function of irradiation time yields k_{TMP}, assuming pseudo-first-order TMP concentration decay. No $^{\bullet}OH$ or $^1O_2$ quenching agents were added in the experiments carried with TMP, based on the conclusions of Lester et al. (2013). These authors carried out TMP degradation experiments in the presence of Suwanee River humic acid (SRHA) under different conditions (in the absence of scavengers; with 50 mmol L^{-1} tert-butanol, with 1 mmol L^{-1} FFA, and after sparging with either O_2 or N_2) and concluded that the reactions of TMP with $^{\bullet}OH$ and $^1O_2$ were insignificant.

AMZ degradation experiments

Additional experiments were performed to evaluate the effect of UW-BOS on AMZ degradation under LP-UV and simulated solar light. These experiments were performed in solutions containing 10 mg L^{-1} of UW-BOS or SRNOM in phosphate buffer. AMZ was spiked to achieve a starting concentration of 2.07×10^{-2} mmol L^{-1}.

Analytical methods

UV-Vis absorption spectra were measured with a Varian Cary 100 Bio spectrophotometer (Agilent) using a 1-cm path length quartz cuvette, in the range 190–820 nm and 1 nm intervals.

Total organic carbon (TOC) was measured using a TOC-VSCH (Shimadzu Corp., Japan) analyzer. The method detection level (MDL) was 0.2 mgC L^{-1}.

An HPLC-UV (Agilent 1200) system equipped with an Agilent Eclipse XDB-C18 (4.6 mm inner diameter × 250 mm, 5 μm) column was used for monitoring AMZ, phenol, pCBA, FFA, and TMP. AMZ concentrations over time during the degradation experiments were determined at 224 nm by gradient elution with a phosphate buffer (pH 2.8)/acetonitrile solution, at a flow rate of 1.0 mL min^{-1}. The following gradient was used: 0–3 min (15% acetonitrile), 3–20 min (15–40% acetonitrile), 20–22 min (40% acetonitrile), 22–23 min (40–15% acetonitrile), and 23–25 min (15% acetonitrile). The mobile phase used to determine pCBA was 45% phosphate buffer (pH 2.8)/55% methanol at a flow rate of 1 mL min^{-1}, with isocratic elution and detection at 234 nm. A flow rate of 1 mL min^{-1} and isocratic elution with 70% phosphate buffer (pH 2.8)/30% methanol was used to monitor FFA at 219 nm. Finally, TMP was monitored at 220 nm, using a phosphate buffer (pH 2.8)/acetonitrile solution as the mobile phase at 1 mL min^{-1}, according to the following gradient elution: 0–6 min (60–80% methanol), 6–10 min (80% methanol), and 10–11 min (80–60% methanol).

Results and discussion

BOS characterization and optical parameters

The absorption spectra of UW-BOS are shown in Fig. 1. For comparison, the spectrum for SRNOM is also presented. The UV-Vis spectra of UW-BOS are featureless, with an exponential decrease with increasing wavelength and extend into the visible. These observations are similar to what is seen for SRNOM (Korshin et al. 1997). On a carbon molar basis, UW-BOSs exhibit slightly higher absorptivities than SRNOM. This is further discussed in the following sections.

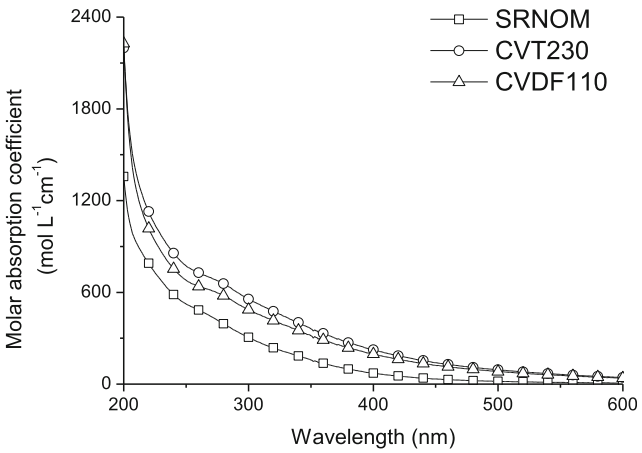

Fig. 1 Absorption spectra of CVT230, CVDF110, and SRNOM measured at a DOC concentration of ~10 mg L^{-1} in 10 mmol L^{-1} phosphate buffer, pH 7.2

The specific UV absorbance at 254 nm ($SUVA_{254}$) for the samples is shown in Table 1. $SUVA_{254}$ is defined as the absorbance of the sample divided by the DOC. $SUVA_{254}$ is an indicator of the amount of aromatic carbon present in the dissolved NOM, which has been shown to be an important indicator of DOC reactivity (Weishaar et al. 2003). The results show that UW-BOS samples exhibit higher $SUVA_{254}$ values and therefore have higher aromaticity than SRNOM. Overall, the $SUVA_{254}$ values for the UW-BOS were generally higher in comparison to values found in the literature for NOM, on average 1.5 times higher (Bodhipaksha et al. 2015; Cawley et al. 2015).

The E2:E3 ratio denotes the ratio of the absorbances at 250 and 365 nm. This parameter can be used as a surrogate for average molecular weight of DOM, decreasing with increasing molecular weight (Helms et al. 2008; Peuravouri and Pihlaja 1997). The calculated E2:E3 ratios for UW-BOS (Table 1) are in agreement with that obtained by Gomis et al. (2015). Based on the $SUVA_{254}$ and E2:E3 values in Table 1 and in the literature, UW-BOS samples appear to be more aromatic and of a higher molar weight than NOM, for which the average E2:E3 ratios are about 4.8 (considering twelve different NOM types) (McKay et al. 2016; Mostafa et al. 2014).

In our case, singlet oxygen formation quantum yields [$\Phi(+^1O_2)$] seem to increase with increasing E2:E3 ratios (Online Resource, Fig. S1), in agreement with previous studies (Mostafa and Rosario-Ortiz 2013). Moreover, this trend was also observed for $\Phi(+^{\bullet}OH)$, the hydroxyl radical formation quantum yield, a result also observed by McCabe and Arnold (2016). (Online Resource, Fig. S2). Analogously, the negative trend of f_{TMP} with E2:E3 suggests that $^3OM^*$ formation increases with increasing E2:E3 ratios (Online Resource, Fig. S3). These results suggest that low-molecular-weight DOM is more photoactive than high-molecular-weight DOM.

The spectral slope (S) was determined from the slope of a plot of $\ln(\alpha_\lambda)$ vs. $(\lambda-\lambda_r)$ according to Eq. 3, where α_λ refers to the linear Napierian absorption coefficients from 300 to 600 nm and λ_r is a reference wavelength (λ_r = 300 nm) (Twardowski et al. 2004). Values of α_λ were calculated according to Eq. 4, where A_λ is the absorbance at wavelength λ and ℓ is the optical path length:

$$\alpha(\lambda) = \alpha(\lambda r)\, e^{-S(\lambda-\lambda r)} \quad (3)$$

$$\alpha(\lambda) = \frac{2.303\ A(\lambda)}{\ell} \quad (4)$$

Both the E2:E3 ratio and the spectral slope are inversely proportional to molecular size (McKay et al. 2016). As obtained for the E2:E3 ratio, the quantum yields of formation of singlet oxygen and hydroxyl radicals seem to increase with increasing spectral slope; the same can be concluded for the formation of $^3OM^*$ (Online Resource, Figs. S4, S5, and S6).

RI quantum yields

Determination of RI formation quantum yields from UW-BOS is of importance to identify the potential use of these materials in water remediation, considering the significant role of reactive species towards the degradation of refractory compounds. Figure 2 summarizes the values of $\Phi(+^1O_2)$, $\Phi(+^{\bullet}OH)$, and f_{TMP} for CVT230 and CVDF110 under simulated solar light and UV radiation. It is worth noting that both UW-BOS samples exhibit similar quantum yields under simulated sunlight, but not under UV irradiation. Similarly to SRNOM, UW-BOS exhibited quantum yields for $^1O_2$ about an order of magnitude greater than those for $^{\bullet}OH$. The quantum yield coefficients for TMP degradation were about a factor of two greater for UW-BOS than SRNOM, both under UV and simulated solar irradiation. Moreover, singlet oxygen is generated with quantum yields three orders of magnitude higher than hydroxyl radical formation, for all types of organic matter. In fact, Vione et al. (2010) found that $^1O_2$ steady-state concentrations were, on average, two orders of magnitude higher than $^{\bullet}OH$ upon irradiation of water from eight different lakes. The authors attribute this fact to the fast formation of $^1O_2$ relative to $^{\bullet}OH$, because the transformation rate constants of $^1O_2$ (10^5 s^{-1}—collision with solvent) and $^{\bullet}OH$ (10^4 to 10^5 s^{-1}—reaction with dissolved compounds) are comparable. It is worth observing that the direct comparison of $\Phi(+^1O_2)$ or $\Phi(+^{\bullet}OH)$ with f_{TMP} is not possible. In fact, $^3OM^*$ is scavenged mostly by dissolved oxygen, and only a small fraction of this species would react with TMP, since a very low concentration of this substrate was used.

UW-BOSs present lower $\Phi(+^1O_2)$ and $\Phi(+^{\bullet}OH)$ and higher f_{TMP} in comparison with values reported for NOM (Cawley et al. 2015; Dalrymple et al. 2010). In fact, under simulated sunlight, the two UW-BOS samples showed $\Phi(+^1O_2)$ and $\Phi(+^{\bullet}OH)$ on average 1.1 and 2.9 times lower than the corresponding values obtained for SRNOM. On the other hand, UW-BOS present f_{TMP} values 2.2 times higher than those obtained for SRNOM. UW-BOSs have a lower efficiency of RI generation compared to SRNOM as determined by

Table 1 DOC concentrations and optical parameters measured for UW-BOS and SRNOM samples

Sample	DOC ($mg_C\ L^{-1}$)	$SUVA_{254}$ ($L\ mg_C^{-1}\ cm^{-1}$)	E2:E3	S (nm^{-1})
SRNOM (1R101N)	6.43	4.22	3.57	0.0125
CVT230	3.96	6.26	2.45	0.0085
CVDF110	3.36	5.49	2.47	0.0084

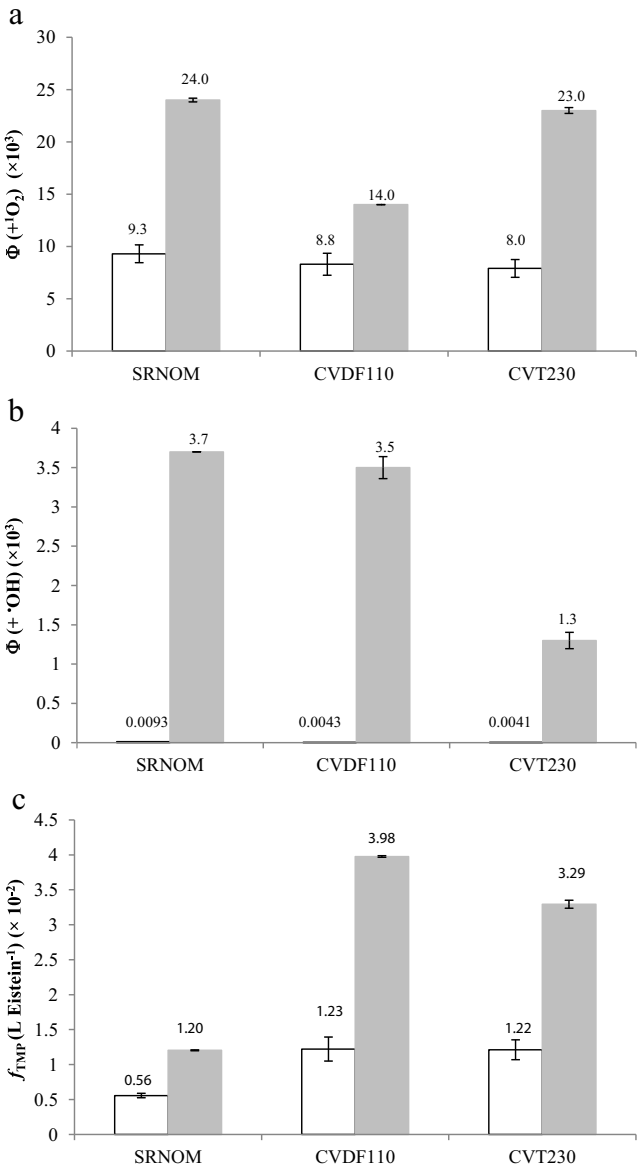

Fig. 2 Quantum yields for (**a**) $^1O_2$ formation, (**b**) $^{\bullet}OH$ formation, and (**c**) quantum yield coefficient of TMP (indicative of $^3OM^*$ formation) from SRNOM and UW-BOS under simulated sunlight and 254-nm UV radiation

measured quantum yields. Although UW-BOS and SRNOM are different in terms of OM source, UW-BOSs are likely higher in aromaticity and molecular weight than SRNOM (see E2:E3 and S values in Table 1). Past research has demonstrated that natural water samples and DOM isolates of various origins exhibit decreasing photoreactivity with increasing molecular weight, which is a potential explanation for the trends observed in this study.

Under low pressure UV irradiation, the values obtained for RI formation quantum yields follow the same trend observed under solar light: the generation of $^1O_2$ and $^{\bullet}OH$ radicals by SRNOM was more efficient in comparison with UW-BOS samples, while UW-BOS degrade TMP more efficiently than SRNOM. Moreover, quantum yields determined with the LP-UV system were greater than those determined with the solar-driven systems. This is consistent with previous work that compared RI quantum yields between simulated sunlight and an LP-UV system (Lester et al. 2013). In our study, for the UW-BOS system under 254-nm irradiation, the quantum yields of $^1O_2$ and $^{\bullet}OH$ formation and the quantum yield coefficient of TMP degradation were on average 2.4, 420, and 2.7 times higher than those observed under simulated solar light, respectively. Although speculative, reasons for increased $\Phi(+^1O_2)$ and f_{TMP} under UV irradiation include excitation into higher energy excited states, a larger fraction of which is able to oxidize TMP and form $^1O_2$. Considering $^{\bullet}OH$, quantum yields under UV irradiation were almost three orders of magnitude greater than those measured with solar irradiation. This could be due to increased direct photolysis of photochemically produced H_2O_2, as well as an increased rate of photoionization of hydroxybenzoic acids, which has been hypothesized to produce $^{\bullet}OH$ (Sun et al. 2015).

Influence on pollutants degradation

Several studies have shown that UW-BOS can enhance pollutant removal. For example, more than 65% removal of 4-chlorophenol was observed in the presence of 100 mg L^{-1} of UW-BOS under simulated solar light (Prevot et al. 2010). Also, 65% removal was achieved for ethyl orange in the presence of UW-BOS under sunlight (Prevot et al. 2011). It is worth mentioning that these pollutants virtually do not undergo direct photolysis (Prevot et al. 2010, 2011). Gomis et al. (2013) reported that the pseudo-first-order reaction rate constants of crystal violet degradation increased from 5.8×10^{-4} to 3.5×10^{-3} min^{-1} in the presence of UW-BOS under

Table 2 Results of photolysis experiments: k, pseudo first-order degradation rate constant; $t_{1/2}$, half-life; and R^2, determination coefficient

	Simulated sunlight				254 nm UV radiation			
	k (h^{-1})	$t_{1/2}$ (h)	% Removal (20 h)	R^2	k (h^{-1})	$t_{1/2}$ (h)	% Removal (2 h)	R^2
SRNOM	3.0×10^{-3}	231	6.4%	0.97	5.4×10^{-2}	12.8	10.7%	0.98
CVT230	3.9×10^{-3}	177	7.9%	0.99	7.2×10^{-2}	9.6	13.1%	0.98
CVDF110	3.5×10^{-3}	198	6.6%	0.96	7.8×10^{-2}	8.9	14.4%	0.98

sunlight. Likewise, an increase in the removals of naphthalene sulfonates from 15 to 30% was obtained when UW-BOS were added to the medium (Avetta et al. 2012). In contrast, Gomis et al. (2014) found that the degradation of a mixture of six emerging pollutants that were prone to direct photolysis was hampered in the presence of UW-BOS. The authors attributed this fact to light screening by these materials.

Peixoto and Teixeira (2014) showed that despite the low molar absorptivity of amicarbazone at 254 nm (ε_λ = 52 L mol^{-1} cm^{-1}), irradiation from LP-Hg lamps can degrade AMZ. For example, the half-life of a neutral pH AMZ solution at $[AMZ]_0$ = 100 mg L^{-1} was ~685 min when irradiated with a 36-W lamp (Peixoto and Teixeira 2014). In our study, amicarbazone-containing solutions were irradiated under simulated sunlight in the presence of SRNOM or UW-BOS in order to compare the contributions of these sources of RI species to herbicide degradation. The results are shown in Table 2. Significant direct photolysis of AMZ under sunlight is unlikely, as reported elsewhere (Silva et al. 2015). Therefore, the solar-driven AMZ degradation is expected to be due to the indirect photolysis promoted by DOM.

AMZ removal followed pseudo-first-order behavior in solutions containing SRNOM or UW-BOS using both simulated sunlight and LP-UV as irradiation sources. Under solar light, a slight increase in AMZ degradation rate was observed in the presence of UW-BOS. On the other hand, for the UV-irradiated system, the AMZ half-lives are on average 1.4 times lower in the presence of UW-BOS. Despite these differences, we would argue that organic matter isolated from urban-bio waste and naturally occurring DOM (i.e. SRNOM) are comparable in terms of their capacities of sensitizing organic pollutants. Considering their application in treatment of polluted waters, conditions required for high removal depend on the type of radiation source used. If mixtures of AMZ and UW-BOS were exposed to solar radiation, increased concentrations of UW-BOS would increase removal rates, because AMZ does not absorb light (and thus undergo direct photolysis) in the solar spectrum. Conversely, if LP-UV radiation is used, it is desirable to have low concentrations of UW-BOS due to light screening of AMZ.

The rate of photo-degradation of a pollutant (P) is the sum of direct and indirect photolysis, the last one mainly by interactions with $^1O_2$, $^\bullet$OH, and $^3OM^*$ (Eq. 5):

$$-r_P = (k_{directphot} + k_{\bullet OH,P}[^\bullet OH] + k_{^1O_2,P}[^1O_2] + k_{^3OM^*,P}[^3OM^*] + k_{others})[P] \quad (5)$$

As a consequence, higher values of $-r_P$ are expected with the addition of UW-BOS for large values of the second-order rate constant $k_{^3OM^*,P}$ since UW-BOS present high values of f_{TMP} (indicative of $^3OM^*$ formation).

Zeng and Arnold (2013) studied the contributions of direct photolysis, $^1O_2$, $^\bullet$OH radicals, $^3OM^*$, and others species to pesticide photo-degradation. For pesticides that were inefficiently degraded by direct photolysis, the authors showed that the indirect photolysis induced by $^3OM^*$ was the dominating process. In effect, the percent contributions of $^3OM^*$ were 66% (atrazine), 55% (cyanazine), 44% (acetochlor), 47% (alachlor), 50% (metolachlor), 62% (mesotrione), 79% (diuron), 67% (isoproturon), and 55% (metoxuron) in surface water samples collected from US Geological Survey (USGS) Cottonwood Lake study area, Jamestown, North Dakota.

Conclusions

In this study, optical properties and reactivity of UW-BOS under solar light and UV irradiation (254 nm) was detailed, which will contribute to understand the potential use of these bio-organic materials in engineered photochemical treatment processes. UW-BOS extracted from gardening-park trimming residues, urban waste, and sewage sludge are capable of generating $^3OM^*$ more efficiently than natural organic matter (NOM), as a result, the presence of UW-BOS could favor the degradation of compounds of environmental concern, like pesticides, which exhibit large second-order rate constants with $^3OM^*$.

Through the assessment of UW-BOS photosensitizing properties and RI formation quantum yields, UW-BOSs were shown to be not necessarily better than naturally occurring DOM, i.e., SRNOM. However, because they do sensitize the production of RI, they could potentially be used in engineered treatment scenarios, from both the economic and ecological point of view. The RI formation quantum yields and quantum yield coefficient values determined in this study from UW-BOS, reported here for the first time in literature, will contribute to estimate the potential of these species in environmental aquatic photochemistry.

Acknowledgments The authors thank the Coordination for the Improvement of Higher Level Personnel (CAPES) for the financial support and also the Science without Borders Program (Process No. 12354/13-9) for the financial support during the internship at the University of Colorado at Boulder, USA. The authors also thank Prof. A. Arques (Universidad Politécnica de Valencia, Spain), Prof. G. Magnaca (Università di Torino, Italy), and Prof. A. Bianco Prevot (Università di Torino, Italy) for the UW-BOS samples (Marie Curie Actions—IRSES International Research Staff Exchange Scheme—269128 Project).

Compliance with ethical standards

Conflict of interest The authors declare that they have no conflict of interest.

References

Arques A, Prevot A (2015) Soluble bio-based substances isolated from urban wastes. Springer International Publishing, ISBN 978-3-319-14744-4 (eBook), DOI 10.1007/978-3-319-14744-4

Avetta P, Prevot AB, Fabbri D, Montoneri E, Tomasso L (2012) Photodegradation of naphthalene sulfonic compounds in the presence of a bio-waste derived sensitizer. Chem Eng J 197:193–198

Avetta P, Bella F, Prevot AB, Laurenti E, Montoneri E, Arques A, Carlos L (2013) Waste cleaning waste: photodegradation of monochlorophenols in the presence of waste-derived photosensitizer. Sustain Chem Eng 1:1545–1550

Avetta P, Berto S, Prevot AB, Minella M, Montoneri E, Persico D, Vione D, Gonzalez MC, Mártire DO, Carlos L, Arques A (2015) Photoinduced transformation of waste-derived soluble bio-based substances. Chem Eng J 274:247–255

Bodhipaksha LC, Sharpless CM, Chin YP, Sander M, Langston WK, Mackay AA (2015) Triplet photochemistry of effluent and natural organic matter in whole water and isolates from effluent-receiving rivers. Environ Sci Technol 49:3453–3463

Bound JP, Voulvoulis N (2004) Pharmaceuticals in the aquatic environment-acomparison of risk assessment strategies. Chemosphere 56:1143–1155

Braun AM, Maurette MT, Oliveros E (1991) Photochemical technology. Wiley, Chischester

Canonica S, Freiburghaus M (2001) Electron-rich phenols for probing the photochemical reactivity of freshwaters. Environ Sci Technol 35: 690–695

Cawley KM, Hakala JA, Chin YP (2009) Evaluating the triplet state photoreactivity of dissolved organic matter isolated by chromatography and ultrafiltration using an alkylphenol probe molecule. Limnol Oceanogr Methods 7:391–398

Cawley KC, Korak JA, Rosario-Ortiz FL (2015) Quantum yields for the formation of reactive intermediates from dissolved organic matter samples from the Suwannee River. Environ Eng Sci 32:31–37

Dalrymple RM, Carfagno AK, Sharpless CM (2010) Correlations between dissolved organic matter optical properties and quantum yields of singlet oxygen and hydrogen peroxide. Environ Sci Technol 44:5824–5829

Dorfman LM, Taub IA, Buhler RE (1962) Pulse radiolysis studies I: transient spectra and reaction-rate constants in irradiated aqueous solutions of benzene. J Chem Phys 36:3051–3061

Emblidge JP, De Lorenzo ME (2006) Preliminary risk assessment of lipid-regulating pharmaceutical clofibric acid, for three estuarine species. Environ Res 100:216–226

Golanoski KS, Fang S, Del Vecchio R, Blough NV (2012) Investigating the mechanism of phenol photooxidation by humic substances. Environ Sci Technol 46:3912–3920

Gomis J, Verchera RF, Amat AM, Mártire DO, González MC, Prevot AB, Montoneri E, Arques A, Carlos L (2013) Application of soluble bio-organic substances (SBO) as photocatalysts for wastewater treatment: sensitizing effect and photo-Fenton-like process. Catal Today 209:176–180

Gomis J, Prevot AB, Montoneri E, González MC, Amat AM, Mártire DO, Arques A, Carlos L (2014) Waste sourced bio-based substances for solar-driven wastewater remediation: photodegradation of emerging pollutants. Chem Eng J 235:236–243

Gomis J, Gonçalves MG, Vercher RF, Sabater C, Castillo MA, Prevot AB, Amat AM, Arques A (2015) Determination of photostability, biocompatibility and efficiency as photo-Fenton auxiliaries of three different types of soluble bio-based substances (SBO). Catal Today 252:177–183

Haag WR, Hoigné J, Gassman E, Braun A (1984) Singlet oxygen in surface waters—part II: quantum yields of its production by some natural humic materials as a function of wavelength. Chemosphere 13:641–650

Helms JR, Stubbins A, Ritchie JD, Minor EC, Kieber DJ (2008) Absorption spectral slopes and slope ratios as indicators of molecular weight, source, and photobleaching of chromophoric dissolved organic matter. Limnol Oceanogr Methods 53:955–969

Korshin GV, Li CW, Benjamin MM (1997) Monitoring the properties of natural organic matter through UV spectroscopy: a consistent theory. Water Res 31:1787–1795

Larson RA, Zepp RG (1988) Reactivity of the carbonate radical with aniline derivatives. Environ Toxicol Chem 7:265–274

Lester Y, Sharpless CM, Mamane H, Linden KG (2013) Production of photo-oxidants by dissolved organic matter during UV water treatment. Environ Sci Technol 47:11726–11733

McCabe AJ, Arnold WA (2016) Seasonal and spatial variabilities in the water chemistry of prairie pothole wetlands influence the photoproduction of reactive intermediates. Chemosphere 155:640–647

McKay GJ, Rosario-Ortiz FL (2015) Temperature dependence of the photochemical formation of hydroxyl radical from dissolved organic matter. Environ Sci Technol 49:4147–4154

McKay G, Couch KD, Mezyk SP, Rosario-Ortiz FL (2016) Investigation of the coupled effects of molecular weight and charge-transfer interactions on the optical and photochemical properties of dissolved organic matter. Environ Sci Technol 50:8093–8102

McKay G, Huang W, Romera-Castillo C, Crouch JE, Rosario-Ortiz FL, Jaffé R (2017) Predicting reactive intermediate quantum yields from dissolved organic matter photolysis using optical properties and antioxidant capacity. Environ Sci Technol. doi:10.1021/acs.est.6b06372

Mostafa S, Rosario-Ortiz FL (2013) Singlet oxygen formation from wastewater organic matter. Environ Sci Technol 47:8179–8186

Mostafa S, Korak JA, Shimabuku K, Glover CM, Rosario-Ortiz FL (2014) Relation between optical properties and formation of reactive intermediates from different size fractions of organic matter. In: Advances in the Physicochemical Characterization of Dissolved Organic Matter: Impact on Natural and Engineered Systems, pp. 159–179

Passananti M, Temussi F, Iesce MR, Previtera L, Mailhot G, Vione D, Brigante M (2014) Photoenhanced transformation of nicotine in aquatic environments: involvement of naturally occurring radical sources. Water Res 55:106–114

Peixoto ALC, Teixeira ACSC (2014) Degradation of amicarbazone herbicide by photochemical processes. J Photochem Photobiol A Chem 275:54–64

Peuravouri J, Pihlaja K (1997) Molecular size distribution and spectroscopic properties of aquatic humic substances. Anal Chim Acta 337: 133–149

Prevot AB, Fabbri D, Pramauro E, Baiocchi C, Medana C, Montoneri E, Boffa V (2010) Sensitizing effect of bio-based chemicals from urban wastes on the photodegradation of azo-dyes. J Photochem Photobiol A Chem 209:224–231

Prevot AB, Avetta P, Fabbri D, Laurenti E, Marchis T, Perrone ME, Boffa V (2011) Waste-derived bioorganic substances for light-induced generation of reactive oxygenated species. ChemSusChem 4:85–90

Richard C, Trubetskaya O, Trubetskoj O, Reznikova O, Afanas'eva G, Aguer JP, Guyot G (2004) Key role of the low molecular size fraction of soil humic acids for fluorescence and photoinductive activity. Environ Sci Technol 38:2052–2057

Rosario-Ortiz FL, Canonica S (2016) Probe compounds to assess the photochemical activity of dissolved organic matter. Environ Sci Technol 23:12532–12547

Schwarzenbach RP, Gschwend PM, Imboden DM (2003) Direct photolysis. In: Winter J 2nd (ed) Environmental organic chemistry. Wiley, Hoboken, pp 611–654

Sharpless CM, Aeschbacher M, Page SE, Wenk J, Sander M, McNeill K (2014) Photooxidation-induced changes in optical, electrochemical, and photochemical properties of humic substances. Environ Sci Technol 48:2688–2696

Silva MP, Mostafa S, McKay GJ, Rosario-Ortiz FL, Teixeira ACSC (2015) Environmental photochemical fate of amicarbazone in aqueous medium: laboratory measures and simulations. Environ Eng Sci 32:730–740

Sun L, Qian J, Blough NV, Mopper K (2015) Insights into the photoproduction sites of hydroxyl radicals by dissolved organic matter in natural waters. Environ Sc Technol Lett 2:352–356

Twardowski MS, Boss E, Sullivan JM, Donaghay PL (2004) Modeling the spectral shape of absorption by chromophoric dissolved organic matter. Mar Chem 89:69–88

U.S. Environmental Protection Agency (2016) Pesticides: health and safety. http://www.epa.gov/opp00001/health/human.htm, (acessed 15.03.16).

Vecchiato M, Argiriadis E, Zambon S, Barbante C, Toscano G, Gambaro A, Piazza R (2015) Persistent organic pollutants (POPs) in Antarctica: occurrence in continental and coastal surface snow. Microchem J 119:75–82

Vione D, Das R, Rubertelli F, Maurino CM, Barbati S, Chiron S (2010) Modelling the occurrence and reactivity of hydroxyl radicals in surface waters: implications for the fate of selected pesticides. Int J Environ Anal Chem 90:260–275

Vione D, Maurino V, Minero C (2014) Photosensitised humic-like substances (HULIS) formation processes of atmospheric significance: a review. Environ Sci Pollut Res 21:11614–11622

Weishaar JL, Aiken GR, Bergamaschi BA, Fram MS, Fuji R, Mopper K (2003) Evaluation of specific ultraviolet absorbance as an indicator of the chemical composition and reactivity of dissolved organic carbon. Environ Sci Technol 37:4702–4708

Zeng T, Arnold WA (2013) Pesticide photolysis in prairie potholes: probing photosensitized processes. Environ Sci Technol 47:6735–6745

Zhang D, Yan S, Song W (2014) Photochemically induced formation of reactive oxygen species (ROS) from effluents organic matter. Environ Sci Technol 48:12645–12653

Zhou H, Lian L, Yan S, Song W (2017) Insights into the photo-induced formation of reactive intermediates from effluent organic matter: the role of chemical constituents. Water Res 112:120–128